모서리 응력 특이도를 고려한 다양한 경계조건의 조합을 갖는 마름모꼴형 평판의 엄밀한 진동 해석

Accrate Vibration Analysis of Rhombic Plates with Various Combinations of Edge Conditions Considering Corner Stress Singularities

김 주 우* 한 봉 구**
Kim, Joo-Woo Han, Bong-Koo

요 지

본 논문은 고정, 단순, 또는 자유 연단 조건의 네 가지의 다른 조합을 갖는 마름모꼴형 평판의 자유진동 데이터를 처음으로 제시한 연구이다. 본 논문의 주된 관점은 마름모꼴 형 평판 둔각모서리의 휨응력의 특이도를 엄밀히 고려하여 해석하는 것이다. Ritz방법을 이용하여 수직진동변위를 두 가지 적합 함수식으로 가정하였다. 힌지와 고정, 자유와 고정, 또는 힌지와 자유인 모서리 응력 특이도의 중대한 영향력이 이해 될 수 있도록 충분히 큰 165° 둔각모서리를 갖는 마름모꼴형 평판에 대하여 엄밀한 무차원 진동수와 수직변동변위의 전형적인 등고선을 제시하였다.

핵심용어 : Ritz방법, 진동, 휨모멘트 특이도, 응력, 마름모꼴형 평판, 진동수, 모드형태

Abstract

This paper offers the first known free vibration data for rhombic plates with four different combinations of clamped, simply supported, and free edge conditions. A cornerstone here is that the analysis explicitly considers the bending stress singularities that occur in the two opposite corners having obtuse angles of the rhombic plates. The Ritz method is used with two sets of admissible functions assumed transverse vibratory displacements. Accurate non-dimensional frequencies and normalized contours of the vibratory transverse displacement are presented for rhombic plates having a large enough obtuse angle of 165°, so that a significant influence of hinged-clamped, free-clamped, and hinged-free corner stress singularities may be understood.

Keywords : *Ritz method, vibration, bending moment singularities, stress, rhombic plates, frequencies, mode shapes*

1. INTRODUCTION

Although a number of researches has been carried out on the free vibration behavior of simply supported skew (rhombic) plates[1)~5)], a search of the literature has revealed that little

* 정회원·서울산업대학교 구조공학과, 강사
** 정회원·서울산업대학교 구조공학과, 부교수

• 이 논문에 대한 토론을 1999년 3월 31일까지 본 학회에 보내주시면 1999년 6월호에 그 결과를 게재하겠습니다.

accurate information has been published on the vibrations of skew or rhombic plates with combinations of clamped, simply supported, and free edge conditions. A recent article[6] used the Ritz method in conjunction with Mindlin plate theory to examine the flexural vibrations of thick skew (and rhombic) plates having several combinations of edge conditions. The evolution of the active research work on the free vibration of skew plates with various combinations of either clamped and simply supported or clamped and free edge condition is described in a summarizing monograph[7] and in subsequent review articles[8)~10].

The shortcoming of the various methods of analysis used in the cited researches is that each has not adequately addressed the unbounded bending stress singularities at the *hinged-clamped, clamped-free, or hinged-free* corners having an interior angle larger than 90° (i.e., obtuse). Essential components of the assumed transverse displacements are corner functions that explicitly account for the unbounded hinged-clamped, clamped-free, or hinged-free corner stresses. These corner functions must be considered in order to avoid erroneous results for rhombic plates having a high degree of skewness. Fundamental stress singularity behavior at obtuse corners in plate flexure problems involving static loads was investigated by Williams[11]. Along these lines, the importance of considering re-entrant corner stress singularities on the natural vibrations of cantilevered skew plates and simply supported rhombic plates has been demonstrated in previous work[12), 13].

This paper describes a continuing investigation into the influence of corner stress singularities on the flexural vibration of rhombic plates. Specifically, the bending stress singularities that exist at the two obtuse interior corners of rhombic plates having four combinations of clamped, simply supported, and free edges are taken into account explicitly. Using the Ritz method, the displacement trial functions consist of a mathematically complete set of algebraic polynomials and two admissible sets of corner functions. The latter functions account for the singular behavior of bending stresses at the two corners having obtuse angles. The strength of singularity increases with increasing corner angle.

The research threads explored in this continuing effort are : (1) to determine whether the stress singularities at the obtuse clamped-hinged, clamped-fee, and hinged-free corners of rhombic plates must be explicitly taken into consideration to obtain accurate vibration solutions; and (2) to present accurate non-dimensional frequencies and normalized displacement contours. Non-dimensional frequency data is presented showing (i) the influence of the corner functions on the upper bound convergence of frequency solutions, and (ii) the effect of skew angle, β, on rhombic plate with various combinations of edge conditions.

2. METHOD OF ANALYSIS

Shown in Fig. 1 is a rhombic plate having typical length, c, and diagonal half-lengths, a and b, measured along the Cartesian axes, x and y, respectively. The vibratory transverse displacement of the rhombic plate is $w=w(x, y, z)$, where t is time. For free vibrations, the temporal dependence of the transverse displacement w is assumed to oscillate cosinusoidally :

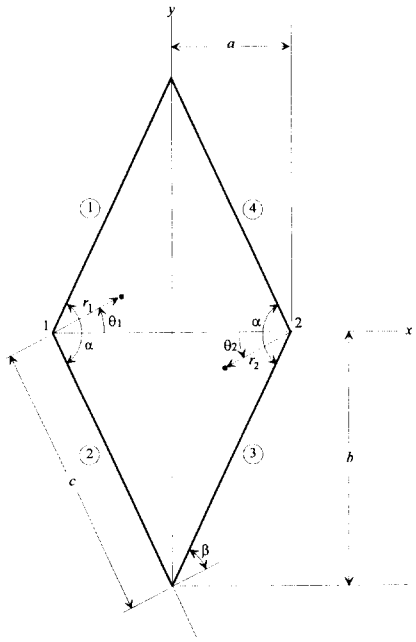

Fig. 1 Geometry of rhombic plates

$$w(x, y, t) = W(x, y)\cos\omega t, \tag{1}$$

where ω is the circular frequency of vibration.

Considering this assumption one can obtain the maximum strain energy due to bending during a vibratory cycle upon :

$$V_{max} = \frac{D}{2}\iint_A [(\chi_x + \chi_y)^2 - 2(1-\nu)(\chi_x\chi_y - \chi_{xy}^2)]dA, \tag{2}$$

where $dA=dxdy$, $D=Eh^3/12(1-\nu^2)$ is the flexural rigidity, h is the plate thickness (not shown in Fig. 1), E is Young's modulus, ν is Poisson's ratio, and χ_x, χ_y and χ_{xy} are the maximum bending and twisting curvatures :

$$\chi_x = \frac{\partial^2 W}{\partial x^2},\ \chi_y = \frac{\partial^2 W}{\partial y^2},\ \chi_{xy} = \frac{\partial^2 W}{\partial x \partial y} \tag{2a}$$

Similarly, the maximum kinetic energy is

$$T_{max} = \frac{\rho\omega^2}{2}\iint_A W^2 dA, \tag{3}$$

where ρ is the mass per unit area of the plate.

In the present Ritz approach, displacement trial functions are assumed as

$$W(x, y) = W_p(x, y) + W_{c_1}(x, y) + W_{c_2}(x, y) \tag{4}$$

where W_p is an admissible and mathematically complete set of algebraic polynomials, and W_{c_1} and W_{c_2} are two sets of corner functions, which adhere to the vanishing displacement and which account for the singular bending stress behavior at the obtuse corners 1 and 2, respectively (see Fig. 1).

Four different combinations of rhombic plate edge conditions are examined, which are hereafter described as *SCFC*, *SCFS*, *SCSF*, and *SCFF* (see Fig. 2, wherein those edges which are simply supported, clamped, or free have been identified by letters *S*, *C*, or *F*). These edge conditions are identified according to the numbered edges shown in Fig. 1 (e.g., *S-C-F-C* corresponding to edges 1-2-3-4 as shown).

Let G_j correspond to the equation of the j^{th} edge of the rhombic plate shown in Fig. 1. Thus,

$$G_1 = b - y + \frac{b}{a}x,\quad G_2 = b + y + \frac{v}{a}x,$$
$$G_3 = b + y - \frac{b}{a}x,\quad G_4 = b - y - \frac{b}{a}x \tag{5}$$

The polynomials W_p are assumed as

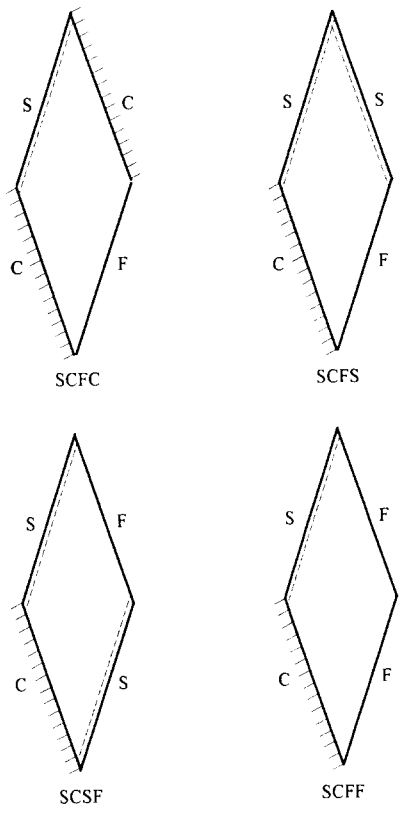

Fig. 2 Rhombic plates having various edge conditions

$$SCFC \text{ plate} : W_p(x, y)=G_1G_2^2G_4^2\phi \tag{6a}$$

$$SCFS \text{ plate} : W_p(x, y)=G_1G_2^2G_4\phi \tag{6b}$$

$$SCSF \text{ plate} : W_p(x, y)=G_1G_2^2G_3\phi \tag{6c}$$

$$SCFF \text{ plate} : W_p(x, y)=G_1G_2^2\phi \tag{6d}$$

where

$$\phi = \sum_{m}^{M}\sum_{n}^{N} A_{mn}x^m y^n \tag{6e}$$

and A_{mn} are undetermined coefficients, m, n $=0$, 1, 2, ..., and W_p satisfies the vanishing displacement and normal slope conditions on all the simply supported and clamped boundaries as required. The corner functions $W_{c_i}(i=1, 2)$ may be written as

$SCFC$ plate :

$$W_{c_1}(x, y)=G_3^2\xi_{1_k},\ W_{c_2}(x, y)=G_1G_2^2\xi_{2_k} \tag{7a}$$

$SCFS$ plate :

$$W_{c_1}(x, y)=G_4\xi_{1_k},\ W_{c_2}(x, y)=G_1G_2^2\xi_{2_k} \tag{7b}$$

$SCSF$ plate :

$$W_{c_1}(x, y)=G_3\xi_{1_k},\ W_{c_2}(x, y)=G_1G_2^2\xi_{2_k} \tag{7c}$$

$SCFF$ plate :

$$W_{c_1}(x, y)=\xi_{1_k},\ W_{c_2}(x, y)=0 \tag{7d}$$

where

$$\xi_{i_k} = \sum_{k=1}^{K} B_{i_k}W^*_{c_{i_k}}(x, y) \tag{7e}$$

in which B_{i_k} are arbitrary coefficients, and $W^*_{c_{i_k}}$ are biharmonic functions, which satisfy the S-C, C-F, and S-F boundary conditions along two radial edges of a sector plate domain[14]. For all of the plate edge conditions, $W^*_{c_{i_k}}$ is the k^{th} function of the set :

$SCFC$, $SCSF$, $SCFS$, and $SCFF$ plates :

$$\begin{aligned} W^*_{c_{i_k}}(r_1, \theta_1) = r_1^{\lambda_k+1}\Big[&\sin(\lambda_k+1)\theta_1 \\ &-\frac{\sin(\lambda_k+1)\alpha/2}{\cos(\lambda_k+1)\alpha/2}\cos(\lambda_k+1)\theta_1 \\ &-\frac{\sin(\lambda_k+1)\alpha/2}{\sin(\lambda_k-1)\alpha/2}\sin(\lambda_k+1)\theta_1 \\ &+\frac{\sin(\lambda_k+1)\alpha/2}{\cos(\lambda_k-1)\alpha/2}\cos(\lambda_k-1)\theta_1\Big] \end{aligned} \tag{8}$$

SCFC plates :

$$W^*_{C_{2k}}(r_2,\ \theta_2) = r_2^{\lambda_k+1}[\sin(\lambda_k+1)\theta_2 - g_{1_k}\cos(\lambda_k+1)\theta_2 + g_{2_k}\sin(\lambda_k-1)\theta_2 - g_{3_k}\cos(\lambda_k-1)\theta_2] \quad (9a)$$

with

$$g_{1_k}=\frac{\mu_{1_k}}{\delta_k},\quad g_{2_k}=\frac{\mu_{2_k}}{\delta_k},\quad g_{3_k}=\frac{\mu_{3_k}}{\delta_k} \quad (9b)$$

$$\mu_{1_k}=(\lambda_k-1)\gamma_{2_k}\sin(\lambda_k+1)\frac{\alpha}{2} - (\lambda_k+1)\gamma_{1_k}\cos(\lambda_k+1)\frac{\alpha}{2}\sin(\lambda_k-1)\alpha + (\lambda_k-1)\gamma_{1_k}\sin(\lambda_k+1)\frac{\alpha}{2}\cos(\lambda_k-1)\alpha \quad (9c)$$

$$\mu_{2_k}=(\lambda_k+1)\Big[\gamma_{1_k}\cos(\lambda_k-1)\frac{\alpha}{2} - \gamma_{2_k}\cos(\lambda_k-1)\frac{\alpha}{2}\cos(\lambda_k+1)\alpha - \gamma_{3_k}\sin(\lambda_k-1)\frac{\alpha}{2}\sin(\lambda_k+1)\alpha\Big] \quad (9d)$$

$$\mu_{3_k}=(\lambda_k+1)\Big[\gamma_{1_k}\sin(\lambda_k11)\frac{\alpha}{2} + \gamma_{2_k}\sin(\lambda_k-1)\frac{\alpha}{2}\cos(\lambda_k+1)\alpha - \gamma_{3_k}\cos(\lambda_k-1)\frac{\alpha}{2}\sin(\lambda_k+1)\alpha\Big] \quad (9e)$$

$$\delta_k=(\lambda_k-1)\gamma_{2_k}\cos(\lambda_k+1)\frac{\alpha}{2} - (\lambda_k+1)\gamma_{1_k}\sin(\lambda_k+1)\frac{\alpha}{2}\sin(\lambda_k-1)\alpha - (\lambda_k-1)\gamma_{1_k}\cos(\lambda_k+1)\frac{\alpha}{2}\cos(\lambda_k-1)\alpha \quad (9f)$$

in which

$$\gamma_{1_k} = \lambda_k(\nu-1)+(3+\nu),\quad \lambda_{2_k}=(\lambda_k+1)(\nu-1),\quad \gamma_{3_k}=(\lambda_k-1)(\nu-1) \quad (9g)$$

SCSF plate :

$$W^*_{C_{2k}}(r_2,\ \theta_2)=r_2^{\lambda_k+1}[\sin(\lambda_k+1)\theta_2 - h_k\cos(\lambda_k+1)\theta_2 - h_2\sin(\lambda_k-1)\theta_2 + h_{3_k}\cos(\lambda_k-1)\theta_2] \quad (10a)$$

SCFS plate :

$$W^*_{C_{2k}}(r_2,\ \theta_2) = r_2^{\lambda_k+1}[\sin(\lambda_k+1)\theta_2 + h_k\cos(\lambda_k+1)\theta_2 - h_2\sin(\lambda_k-1)\theta_2 - h_{3_k}\cos(\lambda_k-1)\theta_2] \quad (10b)$$

with

$$h_{1_k} = \frac{\sin(\lambda_k+1)\alpha/2}{\cos(\lambda_k+1)\alpha/2},\quad h_{2_k} = \frac{\eta_k\sin(\lambda_k+1)\alpha/2}{\sin(\lambda_k-1)\alpha/2}$$

$$h_{3_k} = \frac{\eta_k\sin(\lambda_k+1)\alpha/2}{\cos(\lambda_k-1)\alpha/2} \quad (10c)$$

where

$$\eta_k = \frac{(\lambda_k+1)(\nu-1)}{\lambda_k(\nu-1)+(3+\nu)} \quad (10d)$$

In Eqs. (8)-(10), the are the $(r_i,\ \theta_i)$ local polar coordinates originating at corners 1 and 2 (Fig. 1), and α is the included angle of corner 1 and 2.

In Eqs. (8)-(10), the λ_k are the roots of the characteristic equations :

S-C boundary condition :

$$\sin 2\lambda_k\alpha = \lambda_k\sin 2\alpha \quad (11)$$

C-F boundary condition :

$$\sin^2\lambda_k\alpha = \frac{4}{(1-\nu)(3+\nu)} - \frac{1-\nu}{3+\nu}\lambda_k^2\sin^2\alpha \quad (12)$$

S-F boundary condition :

$$\sin 2\lambda_k\alpha = \frac{\nu-1}{3+\nu}\lambda_k\sin 2\alpha \quad (13)$$

The functions $W^*_{c_k}$, which are ordered by λ_k, are transformed to the global Cartesian coordinates (x, y) through the following relations :

$$r_1 = [(x+a)^2+y^2]^{1/2} \quad \theta_1 = \tan^{-1}[y(x+a)^{-1}],$$

$$r_2 = [(x-a)^2+y^2]^{1/2} \quad \theta_2 = \tan^{-1}[y(x-a)^{-1}] \quad (14)$$

The Ritz minimizing equations are formulated by substituting Eqs. (4)-(10) and (14) into (2) and (3) and taking the partial derivatives :

$$\frac{\partial}{\partial A_{mn}}(V_{\max}-T_{\max})=0, \quad \frac{\partial}{\partial B_{i_k}}(V_{\max}-T_{\max})=0 \quad (15)$$

This results in a set of linear homogeneous algebraic equations involving the constants A_{mn} and B_{i_k}. The vanishing determinant of these equations yields a set of eigenvalues (natural frequencies), expressed in terms of the non-dimensional frequency parameter, $\omega a^2\sqrt{\rho/D}$, which is particularly suitable for the rhombic plate. The frequencies monotonically converge from above to the exact values, as sufficient number of terms in Eq. (4) is used.

Eigenvectors involving the coefficients A_{mn} and B_{i_k} may be determined in the usual manner by substituting the eigenvalues back into the homogeneous equations. Normalized contours of the associated mode shapes may be depicted on a x-y grid in the rhombic plate domain once the eigenvectors are substituted into Eqs. (6e) and (7e).

3. CONVERGENCE STUDIES

Summarized in Tables 1 and 2 are the convergence studies for the first six non-dimensional frequencies $\omega a^2\sqrt{\rho/D}$ of $SCFC$ and SCSF rhombic plates having $b/a=3$(or $\alpha\cong 143^\circ$), respectively. Poisson's ratio (ν) of 0.3 has been used for all calculations in the present analysis. Use of the corner functions W_c along with the polynomials W_p permits one to represent to properly the corner stress singularities in rhombic plate vibrations when they exist. The $(M+1)\times(N+1)$ number of polynomial terms (W_p) shown in Tables 1 and 2 indicates $M+1$ terms retained in the x-direction and $N+1$ terms retained in the y-direction [see Eqs. (6)]. The 2K number of corner functions () define K corner functions used in Eqs. (7) for each of corners 1 and 2.

All of the frequency and mode shapes calculations in this work were performed on an IBM/RISC-6000 Model 970 powerserver with a Model 340 workstation cluster using double precision (14 significant digit) arithmetic. The associate eigenvalue problem is positive definite, and thus the frequency data shown in Tables 1 and 2 were obtained by using a QL algorithm with Cholesky factorization[15),16)].

For large solution determinant sizes $(M+1)\times(N+1)+2K$, the mass operator may become ill-conditioned. Hence, the data marked with a superscript asterisk (*) in Table 2 were obtained by using an algorithm based upon two numerical techniques : (i) a Householder reduction of the dynamical matrices to bidiagonal from with matrix diagonolization achieved by using a QL procedure with shift[15),16)] and (ii) a singular value decomposition technique[17)] using a threshold number of 10^{-25}.

The convergence of frequencies in Tables 1 and 2 shows that by using polynomial terms alone typically results in slow convergence of the upper bound convergence of $\omega a^2\sqrt{\rho/D}$ values. However, the convergence rate of $\omega a^2\sqrt{\rho/D}$ is significantly accelerated when a

Table 1 Convergence of frequency parameters $\omega a^2\sqrt{\rho/D}$ for a *SCFC* rhombic plate ($b/a=3$)

Mode No.	Corner Functions (W_c)	$(M+1)\times(N+1)$ polynomial terms (W_p)						
		8×8	9×9	10×10	11×11	12×12	13×13	14×14
1	0	4.6880	4.6517	4.6286	4.6093	4.5981	4.5873	4.5812
	4	4.5558	4.5544	4.5527	4.5523	4.5519	4.5518	4.5516
	8	4.5537	4.5530	4.5521	4.5519	4.5517	4.5516	4.5516
	12	4.5526	4.5520	4.5518	4.5517	4.5516	4.5516	4.5515
	16	4.5519	4.5518	4.5516	4.5516	4.5515	4.5515	---
2	0	7.3788	7.3540	7.3395	7.3263	7.3177	7.3102	7.3044
	4	7.2726	7.2715	7.2704	7.2701	7.2699	7.2699	7.2698
	8	7.2712	7.2702	7.2700	7.2698	7.2698	7.2698	7.2698
	12	7.2704	7.2699	7.2698	7.2698	7.2698	7.2697	7.2697
	16	7.2699	7.2698	7.2698	7.2698	7.2698	7.2697	---
3	0	10.280	10.199	10.161	10.143	10.125	10.116	10.105
	4	10.143	10.087	10.074	10.070	10.069	10.069	10.068
	8	10.116	10.080	10.072	10.069	10.068	10.068	10.068
	12	10.076	10.070	10.069	10.068	10.068	10.068	10.068
	16	10.074	10.069	10.069	10.068	10.068	10.068	---
4	0	13.700	13.523	13.377	13.335	13.299	13.283	13.267
	4	13.422	13.311	13.225	13.211	13.201	13.200	13.199
	8	13.359	13.291	13.220	13.209	13.201	13.200	13.199
	12	13.294	13.242	13.212	13.204	13.200	13.199	13.199
	16	13.220	13.208	13.201	13.200	13.199	13.199	---
5	0	16.194	16.028	15.919	15.869	15.838	15.816	15.798
	4	15.944	15.812	15.749	15.732	15.730	15.728	15.728
	8	15.892	15.805	15.744	15.731	15.729	15.728	15.727
	12	15.822	15.766	15.734	15.729	15.728	15.727	15.727
	16	15.750	15.736	15.729	15.728	15.727	15.727	---
6	0	19.263	18.620	18.302	18.056	17.991	17.957	17.942
	4	19.006	18.487	18.207	17.983	17.936	17.908	17.904
	8	18.785	18.374	18.154	17.970	17.932	17.907	17.904
	12	18.289	18.097	17.995	17.928	17.916	17.904	17.903
	16	18.142	18.041	17.960	17.922	17.910	17.904	---

--- no results due to matrix ill-conditioning

few corner functions are added to the polynomials. This is mainly attributed to the influence of vibratory bending stress singularities at the obtuse corner 1 and 2 (Fig. 1). For example, using 100 polynomial terms (10×10) without corner functions to represent the fundamental mode of an *SCFC* plate with $b/a=3$ (see Table 1) yields an error of approximately 1.7% in the predicted frequency. Increasing to 196 polynomial terms (14×14) still results in an error of 0.6%. When the trial set of 100 polynomials are supplemented with 4 corner functions the predicted frequency error reduces to a negligible amount of 0.03%. Levels of solution accuracy similar to that exhibited above may be seen in all modes of the

Table 2 Convergence of frequency parameters $\omega a^2\sqrt{\rho/D}$ for a *SCSF* rhombic plate ($b/a=3$)

Mode No.	Corner Functions (W_c)	$(M+1)\times(N+1)$ polynomial terms (W_p)						
		8×8	9×9	10×10	11×11	12×12	13×13	14×14
1	0	2.2835	2.2653	2.2609	2.2516	2.2494	2.2440	2.2427
	4	2.2264	2.2258	2.2252	2.2251	2.2249	2.2249	2.2248
	8	2.2252	2.2249	2.2248	2.2248	2.2248	2.2248	2.2248
	12	2.2248	2.2248	2.2248	2.2248	2.2248*	---	---
	16	2.2248	2.2248	2.2248	2.2248*	---	---	---
2	0	5.2477	5.2255	5.2185	5.2072	5.2036	5.1972	5.1951
	4	5.1790	5.1774	5.1767	5.1765	5.1764	5.1763	5.1763
	8	5.1773	5.1768	5.1764	5.1763	5.1762	5.1762	5.1762
	12	5.1766	5.1764	5.1763	5.1763	5.1762*	---	---
	16	5.1763	5.1762	5.1762	5.1762*	---	---	---
3	0	8.2221	8.1738	8.1531	8.1477	8.1383	8.1361	8.1304
	4	8.1623	8.1150	8.1108	8.1082	8.1077	8.1076	8.1075
	8	8.1469	8.1105	8.1097	8.1076	8.1075	8.1074	8.1074
	12	8.1137	8.1083	8.1078	8.1074	8.1074*	---	---
	16	8.1095	8.1078	8.1076	8.1074*	---	---	---
4	0	11.194	11.166	11.081	11.071	11.037	11.032	11.014
	4	10.995	10.980	10.960	10.959	10.955	10.955	10.954
	8	10.980	10.967	10.958	10.956	10.955	10.954	10.954
	12	10.965	10.957	10.955	10.955	10.954*	---	---
	16	10.957	10.956	10.955	10.954*	---	---	---
5	0	12.322	12.249	12.110	12.094	12.082	12.075	12.072
	4	12.261	12.199	12.063	12.054	12.047	12.046	12.046
	8	12.190	12.157	12.059	12.053	12.046	12.046	12.046
	12	12.134	12.092	12.053	12.051	12.046*	---	---
	16	12.071	12.057	12.047	12.047*	---	---	---
6	0	17.568	16.595	16.536	16.137	16.128	16.090	16.088
	4	17.375	16.562	16.515	16.125	16.119	16.082	16.082
	8	17.220	16.464	16.420	16.118	16.113	16.082	16.082
	12	16.498	16.273	16.149	16.093	16.094*	---	---
	16	16.331	16.134	16.123	16.089*	---	---	---

* singular value decomposition eigenanalysis using a threshold number $=10^{-25}$
--- no results due to matrix ill-conditioning

SCFC and *SCSF* plates (see Tables 1 and 2) and the other boundary condition cases (i. e., *SCFS* and *SCFF* plates which are not shown here for brevity).

4. FREQUENCIES AND MODE SHAPES

Table 3 is a summary of accurate rhombic plate frequencies for the four combinations of clamped, simply supported, and free edges. Listed therein are the first five non-dimensional frequencies $\omega a^2\sqrt{\rho/D}$ (c being the side length, as shown in Fig. 1) of the *SCFC*, *SCFS*, *SCSF*, and *SCFF* rhombic plates having skew angles β (corner angles α) $=15°$ (105°), 30° (120°), 45° (135°), 60° (150°), and 75° (165°). Accurate qualitative modeling of the singular stress phenomena dictates that

Table 3 Frequency parameters $\omega c^2\sqrt{\rho/D}$ for rhombic plates

Skew Angle (α)	α	c/a	Mode No.	SCFC	SCFS	SCSF	SCFF
0°	90°	1.00°	1	23.373*	16.795	12.687	5.3521
				(23.460) +	(16.865)	(12.687)	(5.3639)
			2	35.573*	31.116	33.065	19.077
				(35.612)	(31.138)	(33.065)	(19.171)
			3	62.800*	51.404	41.702	24.675
				(63.126)	(51.631)	(41.702)	(24.768)
			4	66.762*	64.023	63.015	43.093
				(66.808)	(64.043)	(63.015)	(43.191)
			5	77.380*	67.546	72.398	52.708
				(77.502)	(67.646)	(72.398)	(53.000)
15°	105°	1.303	1	24.534	18.342	13.269	5.7114
			2	37.070	32.684	33.443	19.198
			3	66.025	55.291	45.138	28.027
			4	68.005	62.944	62.122	41.967
			5	83.220	75.411	78.873	57.430
30°	120°	1.732	1	28.477	22.326	15.174	6.6327
			2	42.574	37.054	35.948	20.550
			3	71.906	64.768	55.456	35.824
			4	79.456	69.409	64.967	42.467
			5	101.65	92.980	94.554	65.846
45°	135°	2.414	1	37.047	31.183	18.961	8.6992
			2	56.649	47.295	43.497	24.355
			3	85.755	77.413	70.014	45.580
			4	106.35	96.668	84.229	54.699
			5	130.68	116.60	107.23	72.708
60°	150°	3.732	1	57.174	52.738	26.196	13.819
			2	96.416	76.541	62.618	34.517
			3	122.32	110.61	97.139	59.046
			4	165.78	147.29	138.68	87.878
			5	196.02	185.94	146.36	105.63
75°	165°	7.596	1	137.45	134.74	45.634	31.840
			2	229.37	215.43	111.37	74.073
			3	317.87	248.85	188.14	113.46
			4	358.26	323.58	266.19	156.10
			5	445.21	380.39	333.27	203.29

*singular value decomposition eigenanalysis using a threshold number $=10^{-25}$
+ Results in paranthesis cf Leissa[17]

for large $\beta(\alpha)$, a considerable number of corner functions are required at corners 1 and 2 for the *SCFC*, *SCFS* and *SCSF* rhombic plates, and at corner 1 for the *SCFF* plates. Sufficient numbers of polynomials (W_p) and corner functions (W_c) were used to yield at least five significant digit accuracy of the frequencies shown in Table 3. The converged solution sizes used to calculate the frequency data in Table 3 are summarized in Table 4.

It may be seen in Table 3 that as the side length c remains constant $\omega c^2\sqrt{\rho/D}$ increases

Table 4 Number of polynomial and corner function terms required of the five significant figure frequency convergence of Table 3

Edges	β (degrees)	Polynomial terms	Corner functions
SCFC	0, 15, 30	12×12	4
	45	12×12	8
	60	14×14	16
	75	16×16	16
SCFS	0	12×12	0
	15, 30	10×10	4
	45	12×12	4
	60	14×14	12
	75	16×16	16
SCSF	0	10×10	0
	15, 30, 45	12×12	4
	60	14×14	12
	75	16×16	12
SCFF	0	12×12	0
	15, 30, 45	12×12	2
	60	14×14	4
	75	14×14	8

with increasing β, and that the highest frequency values are obtained for the *SCFC* plates, which is to be expected. For all plates, substantial changes in $\omega c^2\sqrt{\rho/D}$ traceable to plate skewness are most distinguishable for $45^\circ \leq \beta \leq 75^\circ$, where one can observe increasingly greater frequency changes as the mode number increases. Frequency solution for the square plates ($\alpha=90^\circ$, $\beta=0^\circ$) are lower upper-bound values compared to those values reported in reference [18], which were obtained by employing the Ritz method with beam eigenfunction approximations of the plate's normal displacement.

Depicted in Figs. 3a and 3b are the vibratory transverse displacement contours corresponding to the least upper bound frequency data for the first six modes listed for *SCFC, SCFS, SCSF*, and *SCFF*. The displacement contours in Figs. 3a and 3b are normalized with respect to the maximum displacement component (i.e., $-1 \leq W/W_{max} \leq 1$, where the negative values of W/W_{max} are depicted as dashed contour lines in Figs 3a and 3b). Non-dimensional frequencies $\omega a^2\sqrt{\rho/D}$ shown in Figs. 3a and 3b correspond to the converged values. Nodal patterns of each mode are shown in Figs. 3a and 3b as slightly darker contour lines of zero displacement W/W_{max} during vibratory motion.

5. CONCLUDING REMARKS

This work presents the first-of-its-kind solutions for free vibrations of classically thin, skewed *SCFC, SCFS SCSF*, and *SCFF* rhombic plates. The Ritz method has been used to determine accurate non-dimensional frequencies. The transverse displacement field has been approximated by mathematically complete polynomials and admissible corner functions that account for the unbounded stresses at the obtuse corners. The feasibility of the above hybrid displacement field has been demonstrated by means of convergence tables. It is shown that poor convergence of frequencies is typically obtained when only polynomial displacement trial functions are used, and that upper bound convergence of solution improves considerably when the hybrid trial sets of polynomials and corner functions are simultaneously utilized.

The first known accurate frequencies and mode shapes for highly skewed ($\beta > 45^\circ$) rhombic plates have been offered here for comparison with future data obtained by other investigators. The message the authors have attempted to convey is that investigators using continuum-based and discrete element-based formulations will have difficulty in obtaining

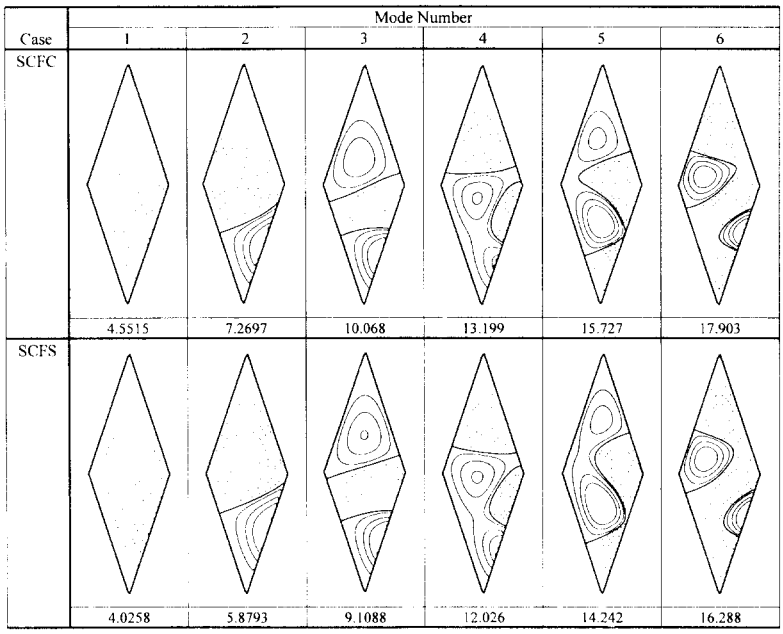

Fig. 3a Normalized transverse displacement contours (W/W_{max}) for the first six modes of *SCFC* and *SCFS* rhombic plates ($b/a=3$)

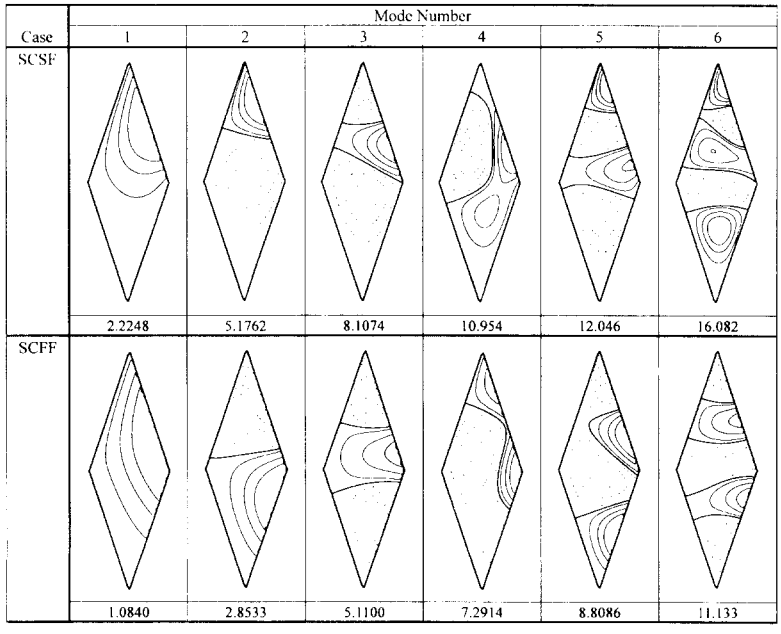

Fig. 3b Normalized transverse displacement contours (W/W_{max}) for the first six modes of *SCSF* and *SCFF* rhombic plates ($b/a=3$)

accurate results unless they explicitly consider in the assumed displacement or stress fields the moment singularities at the obtuse corners.

REFERENCES

1. Durvasula, S., "Free Vibration of Simply Supported Parallelogramic Isotropic Flat Plates", *Journal of Aircraft*, Vol. 6, pp.66~68, 1969.
2. Chopra, I. And Durvasula, S., "Natural Frequencies and Mode Shapes of Tapered Skew Plates", *International Journal of Mechanical Sciences*, Vol. 13, pp.935~944, 1971.
3. Tai, I. H. and Nash, W. A., "Vibration of Thin Plates-a New Approach", *Report No. AFOSR-TR-74-0789*, Department of Civil Engineering, University of Massachusetts, 1973.
4. Sakata, T., "Natural Frequencies of Simply Supported Skew Plates", *International Journal of Mechanical Sciences*, Vol. 23, pp. 677~685, 1981.
5. Gorman, D. J., "Accurate Free Vibration Analysis of Rhombic Plates with Simply Supported and Fully Clamped Edge Conditions", *Journal of Sound and Vibration*, Vol. 125, pp.281~290, 1988.
6. Liew, K. M., Xiang, Y., Kitipornchai, S., and Wang, C. M., "Vibration of Thick Skew Plates Based on Mindlin Shear Deformation Plate Theory", *Journal of Sound and Vibration* Vol. 168, pp.39~69, 1993.
7. Leissa, A. W., "Vibration of Plates", NASA SP-160, U.S. Government Printing Office, 1969. Reprinted, *Acoustical Society of America* (1993).
8. Leissa, A. W., "Recent Research in Plate Vibrations : Classical Theory", *Shock and Vibration Digest*, Vol. 9, pp.13~24, 1977.
9. Leissa, A. W., "Plate Vibration Research 1976-1980 : Classical Theory", *Shock and Vibration Digest* Vol. 13, pp.11~22, 1981.
10. Leissa, A. W., "Recent Studies in Plate Vibrations : 1981-1985 : Part I-Classical Theory", *Shock and Vibration Digest* Vol. 19, pp.11~18, 1987.
11. Williams, M. L., "Surface Stress Singularities Resulting from Various Boundary Conditions in Angular Corners of Plates Under Bending", *Proceedings of the first U.S. National Congress of Applied Mechanics*, pp. 325~329, 1951.
12. McGee, O. G., Leissa, A. W., and Huang, C. S., "Vibration of Cantilevered Skewed Plates with Corner Stress Singularities", International *Journal of Numerical Methods in Engineering*, Vol. 35, pp.409~424, 1992.,
13. Huang, C. S., McGee, O. G., Leissa, A. W., and Kim, J. W., "Accurate Vibration Analysis of Simply Supported Rhombic Plates by Considering Stress Singularities", *ASME Journal of Vibration and Acoustics*, Vol. 151, pp.245~251, 1995.
14. Leissa, A. W., McGee, O. G., and Huang, C. S., "Vibration of Sectorial Plates Having Corner Stress Singularities", *Journal of Applied Mechanics*, Vol. 60, pp.134~140, 1993.
15. Stewart, G. W., *Introduction to Matrix Computation*, New York : Academic Press, 1970.
16. Stoer, J. and Bulirsh, R., *Introduction to Numerical Analysis*, New York : Springer-Verlag, See Article 6.7, 1980.
17. Press, W. H., Flannery, B. P., Teukolsky, S. A., and Vetterling, W. T., *Numerical Recipes-the Art of Scientific Computing*, Cambridge : Cambridge University Press, 1986.
18. Leissa, A. W., "The Free Vibration of Rectangular Plates", *Journal of Sound and Vibration*, Vol. 31, pp.257-293, 1973.

(접수일자 : 1998. 9. 21)